J Mater Sci (2006) 41:5220–5226
DOI 10.1007/s10853-006-0431-y

Design and control of porosity in oxide thin films grown by PECVD

A. Borrás · A. Barranco · A. R. González-Elipe

Received: 8 July 2005 / Accepted: 1 February 2006 / Published online: 29 July 2006
© Springer Science+Business Media, LLC 2006

Abstract This work presents a series of results about the synthesis and characterization of porous oxide thin films (thicknesses ~300 nm) prepared at low temperature by PECVD. Two different experimental strategies are described. A first one, used for the preparation of porous SiO_2 thin films, consists of the use of a polymeric sacrificial layer that is removed during deposition of the oxide thin film. A second one, used for the preparation of TiO_2 thin films, relies on the modification of some critical deposition parameters (i.e., temperature, Ar/O_2 ratio in the plasma mixture, etc.). Thin films with a large variation of pore structures as evidenced by Scanning Electron Microscopy (SEM) have been prepared by the two methodologies. The thin films have been characterised by different techniques and some of their properties related with their microstructure assessed by ellipsometry (optical behaviour) or water contact angle measurements (hydrophobic/hydrophilic character). A quartz crystal monitor has been used to measure water vapour adsorption/desorption isotherms in the films. From the shape of these isotherms it is possible to estimate the type of pores existing in the different thin films. Examples of the potential use of these porous thin films as humidity sensors or hydrophilic surfaces are reported.

A. Borrás · A. Barranco · A. R. González-Elipe (✉)
Instituto de Ciencia de Materiales de Sevilla and Dpt. Q. Inorgánica., CSIC-Univ. Sevilla, Avda. Américo Vespucio s/n, 41092 Sevilla, Spain
e-mail: arge@icmse.csic.es

Introduction

Control of porosity in oxide thin films is extremely important for a wide set of applications. Their employ as antireflection coatings and optical thin films [1, 2], the control of the permittivity in low-k materials [3], their use as membranes [4] and others can be quoted among the ample set of applications that rely on the porosity of oxide thin films. In general, a certain control of porosity in thin films can be achieved by modifying the value of some critical experimental parameters during their synthesis. This approach is generally very straightforward when using sol/gel and similar procedures that involve a heating activation stage to get the final thin film characteristics [5]. Alternatively, the incorporation of sacrificial components that are burned out after the synthesis of the inorganic matrix (i.e., template approach) is a good procedure that is also used for the control of porosity [6]. The fabrication of porous SiO_2 and TiO_2 thin films with ordered mesoporous structures are nice examples showing the feasibility of controlling the porosity in thin films prepared by sol/gel techniques [7, 8]. The use of electrochemical procedures for the synthesis of porous Al_2O_3 membranes from Al foils is another example of this control of porosity in thin films by means of ''wet'' methods [9].

By contrast with these relatively well-defined ''wet'' methodologies, the state of the art for the fabrication of thin films by ''dry'' methods (e.g., evaporation (PVD) or all kinds of activated chemical vapour deposition procedures), has not reached a similar development. Generally, by these methods, porosity develops because of the existence of shadowing effects during the thin film growth and/or because there are condensation

processes in the gas phase. The combination of these factors and the low mobility of the add-species on the surface of the growing thin films when their synthesis is done at low temperatures, usually result in columnar microstructures and high porosities [10]. However, such processes are neither controlled nor fully understood and their reliability for a tailored synthesis of thin films with controlled porosity is far from being an achievement.

The present work reports about some approaches developed in our laboratory to get a precise control of the porosity of oxide thin films prepared at room temperature by plasma-enhanced chemical vapour deposition (PECVD). An advantage of this method in comparison with the classical sol/gel or ceramic procedures is that the thin films are prepared at room or, in general, low temperatures, a characteristic that provides clear advantages when the thin films has to be prepared on temperature sensitive substrates. The first approach investigated in this work consists of the use of sacrificial layers of organic materials that can be removed during the deposition of the oxide thin film. The second approach consists of the adjustment of the deposition parameters (pressure and composition of plasma gas, temperature of support) during deposition. Examples will be shown for TiO_2 and SiO_2 thin films grown under different conditions by using these two methodologies. In the context of this investigation, the microstructure of these thin films will be characterised by Scanning Electron Microscopy (SEM). In addition, it will be shown the high potential of using a quartz crystal monitor (QCM) to measure gas adsorption isotherms in thin films. This technique relies on the same concepts than those of the adsorption isotherms used for the characterization of powder materials [11]. Some examples will be also given about some properties and applications (e.g., optical humidity sensors) of thin films where the porosity is a crucial feature.

Experimental

Thin films of SiO_2 and TiO_2 have been prepared by PECVD in a downstream plasma reactor provided with a SLAN source that can work under ECR (electron cyclotron resonance) conditions. Details about the experimental set-up have been published previously [12].

A $Si(CH_3)_3Cl$ precursor was used for the deposition of SiO_2 thin films. The porous structure of the films was controlled by previously depositing in the same chamber an oxygen rich polymer that acts as sacrificial layer. Toluene was used as precursor of this sacrificial layer. Details about the deposition procedure of this polymeric sacrificial layer can be found in [13]. For the deposition of the SiO_2 thin films, 5 sccm of the silicon precursor and 20 sccm of oxygen were introduced in the plasma reactor that was working under ECR conditions ($P = 2 \times 10^{-2}$ Torr).

A Ti isopropoxide precursor was used for the deposition of the TiO_2 thin films. To dose this precursor into the chamber, oxygen (2.7 sccm) was bubbled at 40 °C through a closed recipient containing that compound. The tubes connecting the precursor recipient and the chamber were conveniently heated at approximately 100 °C to avoid any condensation of the precursor. The plasma source was fed with oxygen or mixtures oxygen plus Argon (total flow of 22 sccm). Final working pressure during deposition conditions was $3\text{–}4 \times 10^{-3}$ Torr.

The microstructure of the thin films was examined by Scanning Electron microscope (Hitachi FESEM S-5200) for specimen deposited on a silicon substrate.

Thickness and refractive index of the films were measured by UV–Vis absorption spectroscopy by using a Lambda 12 UV/Vis (Perkin-Elmer) spectrometer. For the determination of the density of the films, the thickness determined by optical methods or estimated from the SEM micrographs was compared with the mass–thickness determined by X-ray fluorescence (XRF) or Rutherford Back Scattering (RBS). These two methods yielded similar values of mass–thickness within an error bar of about 10%.

Adsorption/desorption isotherms were measured by means of a quartz crystal monitor (QCM) on top of which the porous oxide layer was deposited. The isotherms were obtained by dosing successive amounts of water vapour in a closed chamber where the QCM was located. Previous to the adsorption experiment, the samples were heated at about 120 °C under vacuum to remove the water condensed/adsorbed in the films during their handling in air. To compare the different isotherms, they were corrected by the mass–thickness of the different thin films. Total pore volume was estimated under the assumption that at saturation pressure of the isotherms all the pores were completely filled with water.

Water contact angles were measured with a Cam 100 (KSV) system by leaving a droplet of water (around 1.5 mm size) on the surface of the oxide.

Results and discussion

Pore structure of SiO_2 thin films

As an example of the efficiency of the first type of approach, i.e., the use of a sacrificial organic layer for the control of the thin film porosity, Fig. 1 shows a SEM micrograph corresponding to a SiO_2 sample prepared under standard conditions (i.e., without sacrificial layer) and to a thin film of the same material prepared by using the organic sacrificial polymer (this sample was similar to sample Si–C in Table 1). It is evident from the comparison of the two micrographs, that the thin film prepared by simultaneously removing the sacrificial layers presents a porous microstructure characterized by well-defined columns. The porous characteristics of these thin films can be conveniently modified by adjusting the thicknesses of the sacrificial layers and that of the inorganic material. This tailored synthesis permits the preparation of thin films of quite different densities as evidenced by the data in Table 1 that summarizes information about the preparation protocols of a series of thin films obtained by changing the thickness of the organic layer. It is apparent from the reported data that the density of the films decreases as the relative thickness of the organic sacrificial layers increases.

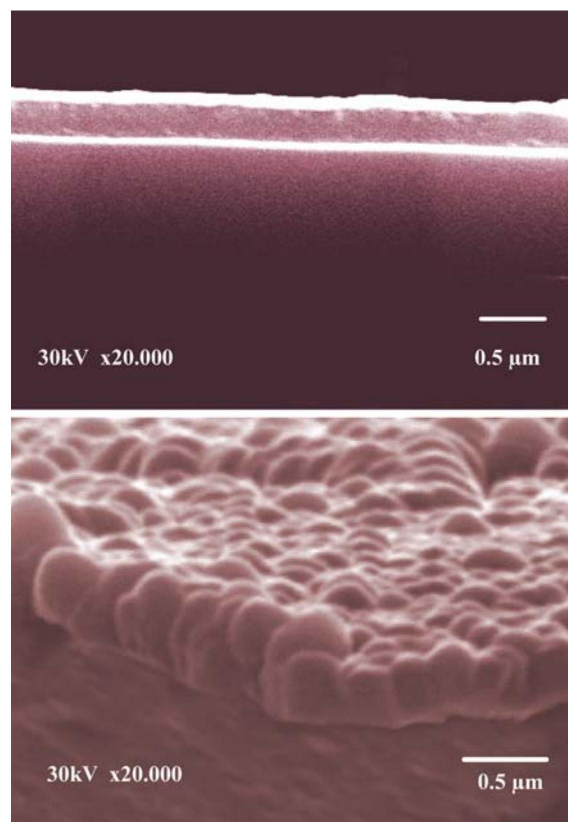

Fig. 1 SEM micrograph of SiO_2 thin films prepared by PECVD by the ‘‘sacrificial layer’’ approach (*bottom*) in comparison with a thin film of this material deposited directly on the substrate

A direct assessment of porosity of thin films is possible by means of water absorption isotherms. This technique is not very common when using a QCM [12, 14], although some authors have reported about its use in combination with their optical characterization by ellipsometry or other means [15]. Figure 2 shows a series of water adsorption isotherms measured on porous SiO_2 thin films prepared by means of PECVD and the sacrificial method. The density of the corresponding thin films and their preparation protocols were as follows: sample Si-H (ρ = 1.65 g/cm^3; 3 steps Pol: 8 nm: SiO_2: 300 nm), sample Si-I (ρ = 1.45 g/cm^3; 4 steps (Pol: 30 nm: SiO_2: 150 nm), sample Si-J (ρ = 1.20 g/cm^3; 3 steps Pol: 50 nm: SiO_2: 150 nm). The shape of these adsorption/desorption isotherms furnishes interesting information concerning the pore structure and total porosity of thin films. Just by looking to the curves in Fig. 2 it is evident that the pore volume follows the order H < J < I. Moreover, the shapes of the isotherms indicate that the majority of pores in sample J are mesopores, while in sample H porosity mainly consists of micropores. In this latter sample the adsorption/desorption process is almost completely reversible. It will be shown below that reversibility is crucial if these thin films are used as sensor elements. The *t*-plots [11] shown in Fig. 2 are derived from the adsorption branch of the previous isotherms and provide a more direct assessment of the type of pores existing in the films [11]. *T*-plots are a useful way for assessing adsorption data which is not restricted to mesoporore sizes as the Kelvin equation [11]. Thus, from the *t*-plot of sample J it is possible to deduce that it mainly consists of mesopores (normalized total pore volume 1.4×10^{-6} cm^3) with a *t*-thickness larger than ~6 Å. By considering the thickness of the water monolayer and the ‘‘core’’ diameter [11], this renders effective pore diameters higher than 38 Å. A similar value was calculated by estimating the pore size distribution by means of the Kelvin equation. In sample Si-I mesopores, with a total pore volume of 1.75×10^{-6} cm^3, are predominant, although some micropores are also present. The micropore volume estimated from the extrapolation of the graph to the *y*-axis is about 0.15×10^{-6} cm^3. Sample Si-H mainly consists of micropores with a volume value of about 0.65×10^{-6} cm^3, estimated by extrapolation of the horizontal plateau-like region of the curve.

Table 1 Preparation protocols of selected porous SiO_2 samples

Sample	Step 1[a]	Step 2[a]	Substrate	Density (g/cm^3)	Porosity (%)
Si-A	SiO_2: 600	–	Si(100)	1.98	10.0
Si-B	Pol.: 25 + SiO_2: 150	Pol.: 25 + SiO_2: 450	Si(100)	1.66	24.6
Si-C	Pol.: 40 + SiO_2: 150	Pol.: 40 + SiO_2: 450	Si(100)	1.25	43.2
Si-D	Pol.: 60 + SiO_2: 150	Pol.: 60 + SiO_2: 450	Si(100)	1.10	55.4
Si-E	Pol.: 60 + SiO_2: 475	Pol.: 60 + SiO_2: 475	Si(100)	1.56	29.4
Si-F	Pol.: 250 + SiO_2: 150	Pol.: 250 + SiO_2: 375	Si(100)	0.78	64.5

[a]Thicknesses in nm

Pol. refers to the thickness of the sacrificial layer and SiO_2 to the thickness of the oxide

Porous SiO_2 thin films as optical sensors

Among the wide set of potential applications of porous thin films that are still transparent (light scattering may occur when the pore size and density are high enough), its employ as optical sensors is an obvious possibility. To check this, we have followed by ellipsometry the optical response of a porous layer similar to the sample H where the adsorption/desorption processes was almost completely reversible and the hysteresis loop was negligible. It is worth noting that the response of a porous thin film for sensor applications would not be reproducible if some gas/vapours become incorporated irreversibly within the pores of the thin films. Figure 3 shows the ellipsometric response of a SiO_2 porous film located in a closed environment where the content of water vapour was adjusted from low to high relative humidity values. The changes are produced because the adsorption of water in the pores of the films modifies its optical constants [15]. It is particularly interesting in Fig. 3 that the large changes in the intensity of the features at ~0.41, ~0.49 or ~0.52 μm as a function of the relative humidity of the air follows a linear relationship (see the right panel in this figure as example). This linear correlation and the reversibility of these changes confer to this thin film the possibility to be used as an optical humidity sensor.

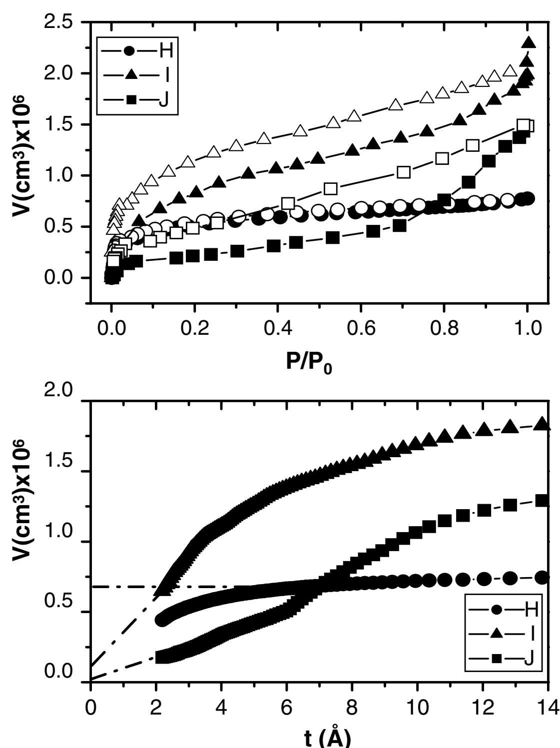

Fig. 2 Water absorption isotherms of SiO_2 thin films with different porosities grown by modifying the thickness of the sacrificial layer (*top*). *t*-plots derived from the previous isotherms (*bottom*)

Microstructure of TiO_2 thin films

Porosity of thin films prepared by PECVD can also be controlled by modifying some significant deposition parameters [1]. We have considered this approach with TiO_2 thin films. An example of the different morphologies that can be obtained is reported in Fig. 4 showing three SEM micrographs of some of the thin films of this material prepared under different conditions as described in Table 2. Refractive indexes of these thin films, taken as a measurement of their density are also reported in this table. The most remarkable effect evidenced by the data in this table in comparison with the SEM micrographs in Fig. 4 is that the films presenting a columnar structure are not necessarily those having the lowest value of refractive index. In fact, the micrograph of sample Ti-B would indicate that it is very compact. By contrast, the refraction index of this sample (i.e., 1.94) is smaller than those of samples Ti-A and Ti-C (i.e., 1.98 and 2.14, respectively). The water adsorption isotherms of the three samples reported in Fig. 5 provide an explanation to this apparent contradiction. In fact, these isotherms confirm that the total pore volume of these thin films follows the order Ti-B > Ti-A > Ti-C (i.e., respective values of 0.85, 0.78 and 0.2×10^{-6} cm^3), in agreement with the tendency of the refractive indexes for these three samples reported in Table 2. Moreover, from the shape of the adsorption isotherms

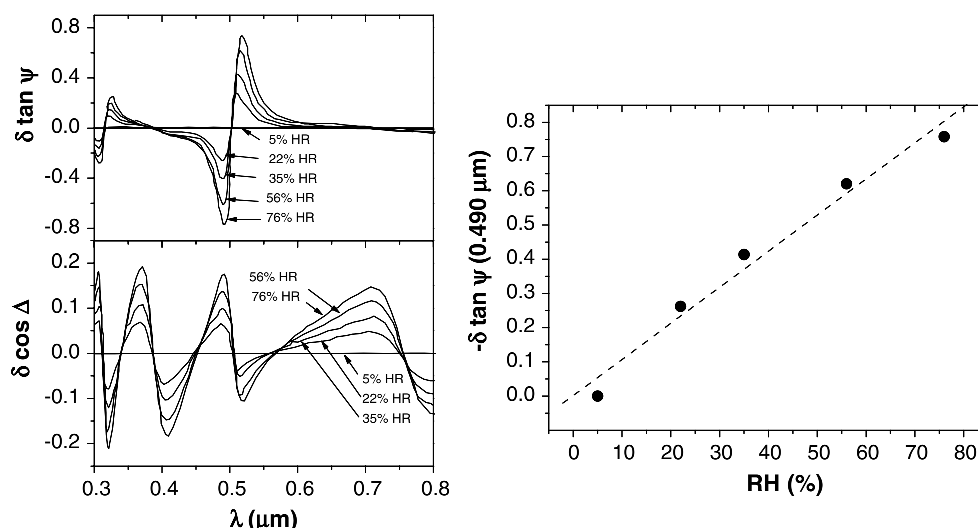

Fig. 3 Ellipsometer response of a porous thin film with a reversible adsorption/desorption cycle as a function of the relative humidity of the air (*left*). Evolution of the intensity of the feature at 0.49 μm with the relative humidity of the air (*right*)

and the ''*t*-plots'' represented in the same figure it is apparent that micropores are predominant in sample Ti-B and mesopores in samples Ti-A and Ti-C, although in the former case micropores also contribute to the porosity with a micropore volume, estimated by extrapolating the *t*-plot curve to the *y*-axis, of 0.22×10^{-6} cm^3. The large hysteresis observed in the adsorption/desorption isotherms of sample Ti-A further confirms a complex porous structure where the adsorbed water remains easily trapped at least that the sample is not heated at $T > 373$ K. On the other hand, the minimum size of the mesopores present in samples Ti-A and Ti-C, estimated from the *t*-plot crossover point at ca. 4 Å, is about 15 Å [11]. By comparing samples Si-J and Ti-C, both mainly consisting of mesopores, it is interesting that the size of pores yielding irreversible condensation is smaller in the TiO_2 than in the SiO_2 samples. This difference should be attributed to the different procedures of preparation used in the two cases.

Optical constants of TiO_2 thin films and water contact angles

The different microstructures of these TiO_2 thin films give rise to significant differences in their properties. Changes in refractive indexes have already been mentioned and summarised in Table 2. It is apparent in this table that the refraction indexes increase with the deposition temperature and are also affected by the presence of Ar in the plasma gas. In this line, the SEM images and water adsorption isotherms reveal that the microstructure of these thin films is also quite different.

Another property that is known to be dependent on the morphology of surfaces is the water contact angle [16]. In general, hydrophobic or hydrophilic materials can be prepared by either a chemical or a topographic modification of their surfaces. For the TiO_2 thin films prepared in the present work we have investigated the evolution of the water contact angle as a function of the temperature of preparation. The results are reported in Fig. 6. This figure shows that the water contact angle decreases from around 100° to 13° for thin films that have been prepared between 298 and 523 K. In the absence of UV illumination, the TiO_2 is typically a hydrophobic material (i.e., water contact angles of about 100° [17]). However, our results in Fig. 6 reveal that it can be made hydrophilic when prepared by PECVD in the form of a thin film at 523 K. Under these conditions, the SEM characterization in Fig. 4 shows that the microstructure of the films may acquire a very particular form characterized by a peculiar columnar microstructure. At the surface, this microstructure renders a very particular surface topography. This is evidenced by the AFM images in Fig. 7 clearly showing that the surface morphology for the samples grown at 298 and 523 K is quite different. In this latter case the surface topography is characterized by two different domain arrangements of approximate length scales of 20 and 300 nm. By contrast, the situation is different for the surface of the sample prepared at 298 K where randomly oriented grains of about 20–40 nm are present in the surface.

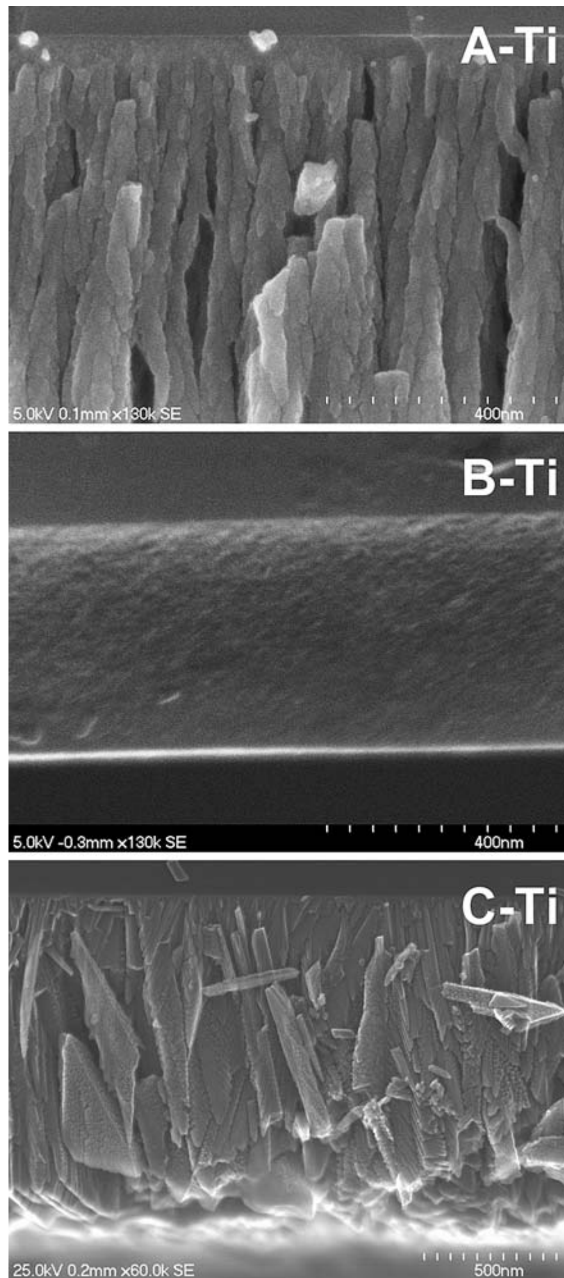

Fig. 4 SEM micrographs of a series of TiO_2 thin films prepared by PECVD under different conditions (see text for details)

Table 2 Preparation conditions and refraction indexes of TiO_2 thin films

Sample	Preparation conditions[a]	Refraction index[b]
Ti-A	298 K, 100%	1.98
Ti-B	298 K, 10%	1.94
Ti-C	523 K, 10%	2.14
Ti-D	500 K, 20%	2.22
Ti-E	500 K, 20%	2.40

[a]Conditions of substrate temperature and percentage of O_2 in the plasma mixture are reported in this column

[b]Refraction indexes measured at 550 nm

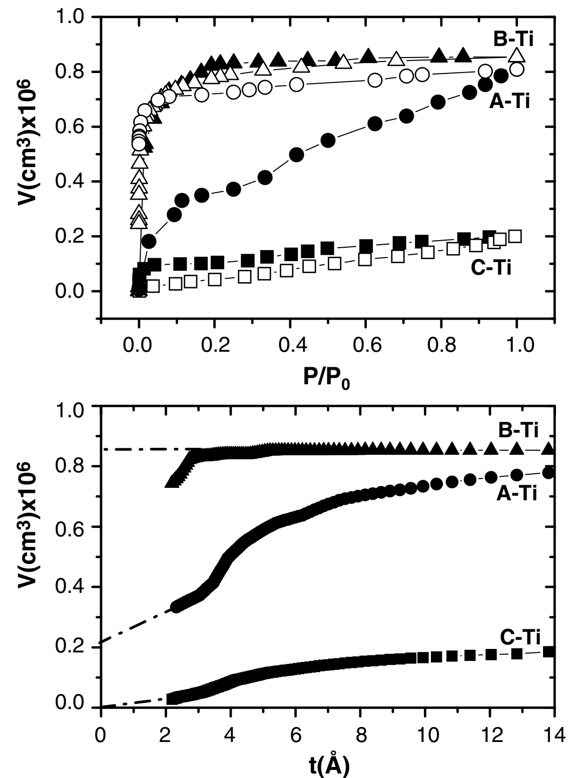

Fig. 5 Water adsorption isotherms of the TiO_2 thin films whose micrographs are reported in Fig. 4 (*top*). *t*-plots derived from the previous isotherm (*bottom*)

Previous reports in the literature concerning the control of the hydrophobic/hydrophilic character of surfaces of other oxide materials like SiO_2, indicate that the type of roughness is a critical factor for the control of the water contact angle [16]. The present results prove that a similar control is possible with thin films of TiO_2 prepared by PECVD by changing the experimental parameters of synthesis.

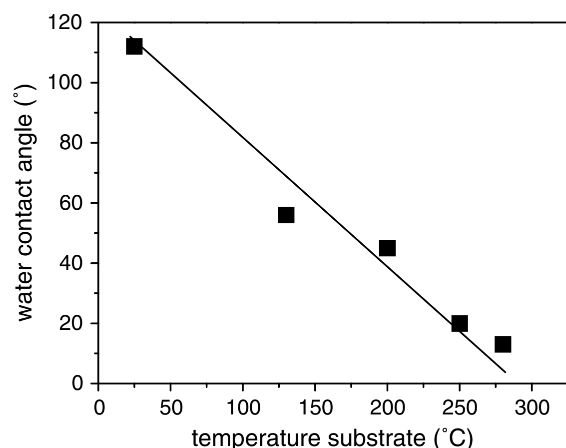

Fig. 6 Evolution of the water contact angle with the temperature of preparation of TiO_2 thin films

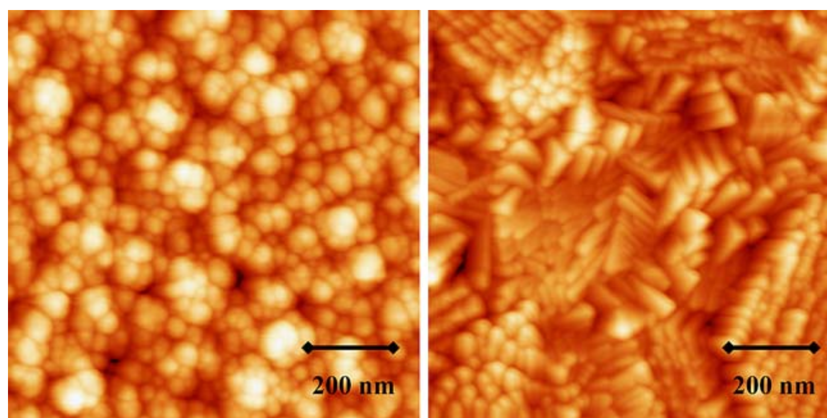

Fig. 7 AFM images of TiO_2 samples prepared at room temperature and at 523 K with a mixture of O_2 (10%) and Ar in the plasma gas

Conclusion

The present investigation has shown that it is possible to control the porosity of oxide thin films prepared by PECVD. Two strategies for an effective control of porosity have been developed. Porosity in SiO_2 thin films can be controlled by depositing an organic sacrificial layer that is easily removed during the plasma deposition of the oxide. Up to a certain oxide thickness, the final porosity of the oxide depends on the thickness of this organic layer. Thicker films can be prepared by successive cycles of organic plus inorganic thin film depositions. Porosity of TiO_2 thin films can be adjusted by modifying the deposition conditions. Temperatures above 473 K and the addition of Ar to the plasma gas are conditions that contribute to enhance the columnar growth of these thin films.

Besides the direct observation by SEM, a quantitative evaluation of the porous structure of the thin films is possible by measuring water adsorption/desorption isotherms. In this way, it has been possible to evidence that thin films with a similar density may have pores of quite different sizes, from micropores to mesopores. Depending on the pore structure of the thin films, different applications can be found for these materials. Examples are shown of their use as optical humidity sensors or for surfaces with controlled hydrophilicity.

Acknowledgments We thank the Ministry of Science and Education of Spain for financial support (project MAT 2004-01558) and A. Álvarez from INTA (Spain) for the ellipsometric characterization of the porous SiO_2.

References

1. Nagel H, Metz A, Hezel R (2001) Solar Energy Mater Solar Cells 65:71
2. Dultsev FN, Solowjev AP (2002) Thin Sol Films 419:27
3. Ruud Balkenende A, de Theije FK, Koen Kriege JC (2003) Adv Mater 15:139
4. Liu P, Lee S-H, Tracy CE, Yan Y, Turner JA (2002) Adv Mater 14:27
5. Lakshmi BB, Dorhout PK, Martin ChR (1997) Chem Mater 9:857
6. Lakshmi BB, Patrissi ChJ, Martin ChR (1997) Chem Mater 9:2544
7. Lu Y, Garguli R, Drewien CA, Anderson MT, Brinker CJ, Gong W, Guo Y, Soyez H, Dunn B, Huang MH, Zink JI (1007) Nature 389:364
8. Vogel R, Meredith P, Kartini I, Harvey M, Riches JD, Bishop A, Heckenberg N, Trau M, Rubinsztein-Dunlop H (2003) Chem Phys Chem 4:595
9. Li FY, Zhang L, Metzger RM (1998) Chem Mater 10:2470
10. González-Elipe AR, Yubero F, Sanz JM (2003) Low energy ion assisted film growth imperial. College Press, London, p 113
11. Gregg SJ, Sing KSW (1982) Adsorption, surface area and porosity. Academic Press, London
12. Barranco A, Cotrino J, Yubero F, Espinós JP, González-Elipe AR (2004) J Vac Sci Technol A 22:1275
13. Barranco A, Cotrino J, Yubero F, González-Elipe AR (2003) J Vac Sci Technol A 21:1655
14. Dultsev FN, Baklanov MR (1999) Electrochem Soild State Lett 2:192
15. Alvarez-Herrero A, Guerrero H, Bernabeu E, Levy D (2002) Appl Optics 41:6692
16. Wu Y, Sugimura H, Inoue Y, Takai O (2002) Chem Vap Deposit 8:47
17. Miyauchi M, Kieda N, Hishita Sh, Mitsuhashi T, Nakajima A, Watanabe T, Hashimoto K (2002) Surf Sci 511:401